ELSEVIER

Solar Energy Materials and Solar Cells 38 (1995) 57–71

Solar Energy Materials and Solar Cells

Absorptivity as a predictor of the photoluminescence spectra of silicon solar cells and photosynthesis

Greg P. Smestad *,[1]

Paul Scherrer Institute, CH-5232, 104-1, Villigen-PSI, Switzerland

Abstract

Experimental photoluminescence spectra obtained for silicon are compared to predictions made using transmission and reflection data, as well as those using the action (or induced photo-product) spectrum. Although the absorptivity obtained from the optical measurements can be used to predict much of the photoluminescence curve, the predicted values may deviate from measurements at long wavelengths. The photoluminescence spectrum for Si, and for photosynthesis found in green plants, may also be predicted from action spectra. Both techniques yield a reasonable fit to the experimental spectral distribution and the predicted chemical potentials and voltages are consistent with electrical measurements.

1. Introduction

The process of quantum solar conversion involves the creation of an excited state via the absorption of light. This photon induced excitation may produce work in an external electrical load, or it may decay to dissipate the excitation energy as heat or light. In a solar cell, the excitation takes the form of an electron-hole pair that is separated in order to produce an external current and voltage. In photosynthesis, the spatially separated electrons may reduce compounds which lead to the fixation of CO_2 and to the storage of fuels. It is therefore desirable to relate the optical properties of a quantum solar converter to the voltages and driving forces generated by the converter. In this way, thermodynamic based predictions of the converter performance can be made [1–5]. Predictions are, in part, possible due to

* Corresponding author.

[1] Current address: Lawrence Berkeley Laboratory, University of California, Energy and Environment Division, Building Technologies Program (MS 62-203), Berkeley, CA, 94720, USA.

SSDI 0927-0248(94)00215-0

Kirchhoff's law which states that the absorptivity, $a(e)$, (the fraction of the incoming light absorbed at some photon energy, e) is equal to the emissivity, $\epsilon(e)$ (the term which describes the ideality of an emitter of light) [6,7]. Previous work by other authors has established that the luminescent emission from an organic or inorganic absorber may be predicted from the optical absorption in the material and that the chemical potential, μ, generated by this light absorption together with temperature determine the strength of the emission [6,8,9]. In addition, it has been demonstrated that the resulting Generalized Planck equation can be applied to silicon and GaAs in order to predict the maximum voltages generated in solar cells [8,9]. Several researchers have applied this concept to photochemical solar converters and to photosynthesis [10–13]. The application of these theoretical concepts to practical systems is not always straightforward. There are several underlying difficulties, the most vexing of which is the determination of the absorptivity at wavelengths where luminescence occurs. This paper will, therefore, examine the experimental application of the Generalized Planck equation to a silicon solar cell and to photosynthesis in order to highlight these difficulties and to suggest directions for future work.

2. Experimental procedure

2.1. Procedure for silicon

The silicon used in this study was a boron doped p-type Siltec wafer which had a resistivity of 15 $\Omega \cdot$ cm. The wafer was coated with a thermally grown SiO_2 passivating layer which also served as an anti-reflecting layer in the visible and near IR (infrared) and gave the wafer a deep blue appearance. The thickness of the SiO_2 was determined, at 70 degrees incidence, to be 0.105 microns by a MOSS model ES4G Sopra ellipsometer (see [14] for experimental technique). The absorptivity was calculated from the wafer thickness, t, absorption coefficient, $\alpha = \alpha(e)$, given by Tiedje et al. [15], and the measured reflection coefficient, Ref_1. This relationship is given by [16]

$$a(e) = [1 - \exp(-\alpha t)] \frac{1 - \mathrm{Ref}_1}{1 - \mathrm{Ref}_1 \exp(-\alpha t)}. \tag{1a}$$

The absorptivity was also estimated from transmission and reflection measurements. Transmission and reflection were measured with an Instrument Systems, Spectra 320 portable spectrometer [17] or a Perkin-Elmer, Lambda 19 double beam spectrophotometer. The general experimental set-up for these measurements is shown in Fig. 1a. Additional optical measurements were taken with a Bomem DA8 002 FTIR (Fourier Transform Infrared) spectrometer equipped with InSb and HgCdTe detectors, a quartz window and glowbar light source. The resolution of the FTIR instrument was 4 cm^{-1}.

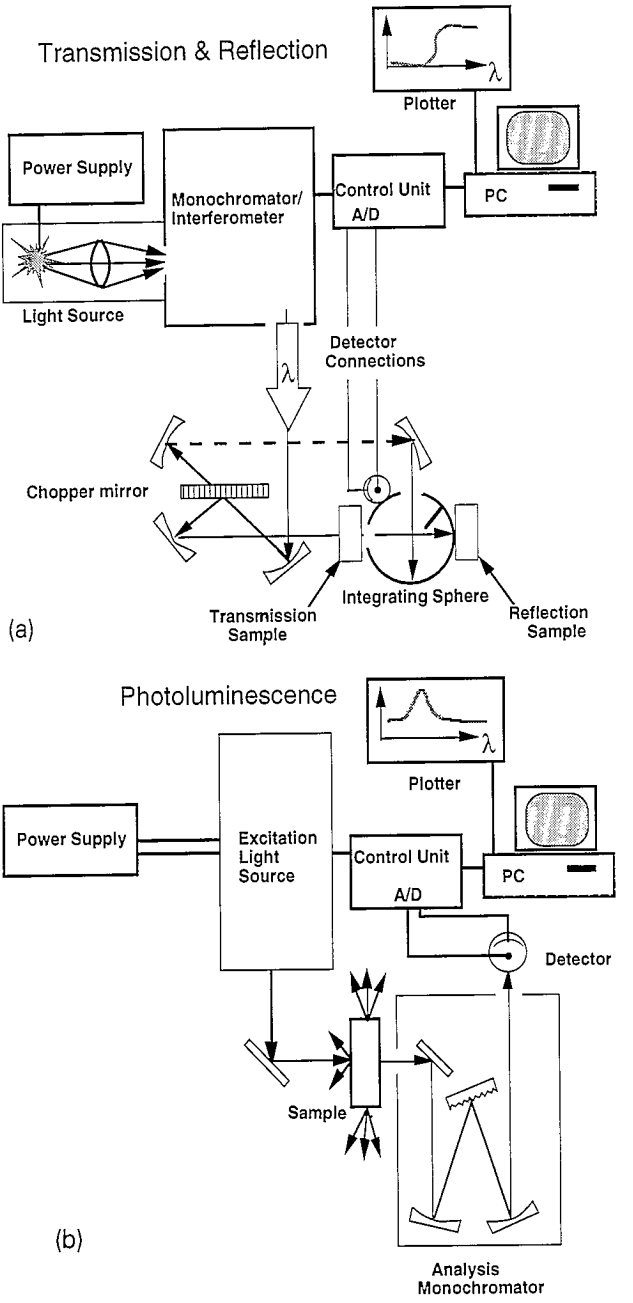

Fig. 1. (a) Experimental set-up used to determine transmission and reflection. Shown is the sample placement for transmission and reflection for the double beam arrangement found in the Perkin Elmer Lambda 19. (b) Experimental set-up used to determine the photoluminescence of a silicon solar cell and a photosynthetic plant leaf. Excitation via a laser induces photoluminescence which is coupled into the analysis monochromator. The measurement unit represents the Instrument Systems Spectro 320 spectrophotometer. (c) Set-up for the determination of solar cell photocurrent spectra. A chopped monochromatic signal produces a photocurrent through, and voltage across, the resistor. The voltage is read by the lock-in amplifier referenced to the chopper frequency. A continuous white light bias is applied to the cell to allow operation near solar illumination levels.

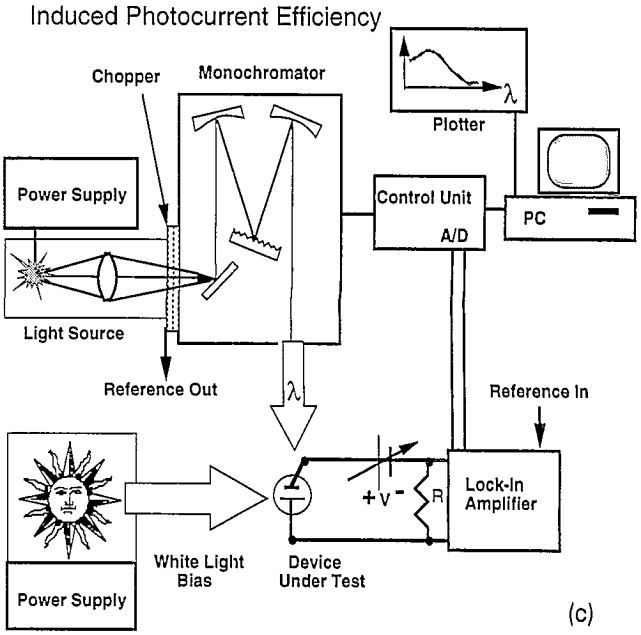

Fig. 1. continued

Photoluminescence was induced using a cw (continuous wave) Argon ion laser (at 514 nm and 488 nm) and recorded using the Instrument Systems, Spectro 320 spectrometer. This commercial instrument consists of one visible and one IR single grating monochromator, a 610 nm long wavelength pass filter, a detector-amplifier package and fiber optic based optical coupling. A thermoelectrically cooled InGaAs photodiode recorded the IR signal, while a Hamamatsu A1547 multi-alkali photomultiplier was used for the visible wavelength range. The Argon laser power was 40 mW, the step size of the instrument was 10 nm and the average scan time was 200 seconds. Factory specified optical sensitivity and detection limit is 50 pW. The photoluminescence experimental set-up is shown in Fig. 1b. In addition to the cw measurements, time resolved photoluminescence measurements were undertaken in order to study the kinetics of the luminescent emission. These time resolved measurements employed a liquid nitrogen cooled Au:Si detector. Excess carriers were produced by 4 ns FWHM (Full Width Half Maximum), 10 Hz repetition rate pulses of a Nd:YAG laser at 532 nm (56 $\mu J/cm^2$). Time resolved detection was made possible by using a Tektronix, 7912AD digitizer and preamplifier which allowed a sweep of the Au:Si detector photocurrent with a time constant of a few nanoseconds. Collection of the photoluminescent emission was aided by the use of a mirrored ellipsoid. This permitted the focusing of the light emitted from the wafer located at the first focus of the ellipsoid to the detector placed at the second focus. The laser spot incident on the silicon wafer was 0.5 mm (FWHM) in diameter for both time resolved and cw measurements.

Absorptivity was also estimated from the induced photocurrent efficiency (IPCE). This measurement was performed using a tungsten halogen light source, Schott OG580 (650 nm) and RG750 (860 nm) long wavelength pass filters, a Bausch & Lomb monochromator, Ithaco 391A Lock-in amplifier and chopper (at 100 Hz). Calibration was accomplished using a Molectron P1 pyroelectric detector. The IPCE set-up is shown in Fig. 1c.

The current–voltage, I–V, curves for a Si solar cell were taken using an Oriel 68820 AM 1.5 Solar simulator which produced an irradiance of 1000 W/m^2 in an area 100×100 mm^2. The apparatus was similar to that shown in Fig. 1c, only the lock-in and monochromator was omitted. The solar cell tested employed a p-type base layer of similar composition to that used in the optical studies.

For both the silicon and photosynthesis study, the chemical potential of the excitation, μ, was used as an adjustable parameter to match the magnitude and photoluminescence efficiency of the predicted curve to that of the measurement. The shape of the predicted photoluminescence curve is established by the measured quantum absorptivity [6,10] using the Generalized Planck equation

$$L(e,\mu,T_0) = a(e)\frac{2n^2}{h^3c^2}\frac{e^3}{\exp\dfrac{(e-\mu)}{kT_0}-1}, \tag{1b}$$

where L is the spectral radiance and T_0 is the ambient temperature. To obtain the flux or number of photons, one divides Eq. (1b) by the photon energy, e. The constant n is the index of refraction of the medium in which the solid angle is measured. The constants h and c are Planck's constant and the speed of light in vacuum, respectively. The constant k is Boltzmann's constant.

2.2. *Experimental procedure for photosynthesis*

The absorption and photosynthetic (photo-product) yield for a leaf was calculated using digitized data from the literature [18]. The photo-product data is given as an average from several crop species, but the yield from many species is similar. In order to convert this to electrons utilized per input photon (which is equivalent to the IPCE used for solar cells) one utilizes the assumption that four photons (electrons) are needed by each of the two photosystems for each molecule of CO_2 reduced. Due to the need for cyclic photosynthetic ATP (Adenosine triphosphate) formation, there is currently some disagreement as to whether 4 or 5 photons are needed [19,20]. If the maximum photosynthetic yield is 0.074–0.09 CO_2 (or O_2) per absorbed photon, then the maximum quantum yield should be eight times this, or 0.6–0.7. This value is used to convert the yield data from values in the literature [18] to those used in this study. In addition, the yield versus wavelength is traditionally reported as the O_2 or CO_2 production per **absorbed** photon, and so the product of the total absorptivity and converted yield per absorbed photon equals the yield per input photon. It is this quantity which is used in this study as the quantum absorptivity for photosynthesis. The leaf total absorptivity data come

from a *Bursera simaruba* leaf [18] measured with an integrating sphere apparatus similar to that shown in Fig. 1a.

As mentioned above, there exists two photosystems in photosynthesis found in green plants (Photosystems II and I, or PSII and PSI). Each photosystem produces it's own distinct spectral shape and possesses accessory pigments and carotenoids which may collect or dissipate energy [19,21]. The photo-product yield for each of these two photosystems was therefore digitized from the work of Joliot [22] on isolated chloroplasts. This allowed for the prediction of the spectral shape and chemical potential for each photosystem.

3. Experimental results

3.1. Results for silicon

Using the absorption coefficient data published for silicon [15], together with Eq. (1a), the absorptivity for the silicon wafer may be calculated. This result is shown in Fig. 2a, together with the photoluminescence curve obtained in the current experimental study. The shape and position of the curve is consistent with the bandgap of silicon (1.12 eV) and the photoluminescence results found in the literature [8,9]. Utilizing the absorption displayed in Fig. 2a, the luminescence predicted from Eq. (1b) is shown in Fig. 2b together with the results of the measurement. The thickness of the wafer displayed in these two figures is indicated as 500 microns. Given the absorption coefficient of silicon at 510–530 nm, one can calculate that only the first 1–2 microns is involved in the initial generation of light. Subsequent propagation of this photoluminescent emission through the wafer will modify the shape of the emitted spectrum depending on the thickness and measurement geometry. In order to explore the effects of thickness on the optical properties, the transmission and reflection spectra of Si wafers of various thicknesses were measured using the Perkin-Elmer spectrophotometer. These results are shown in Fig. 3, and demonstrate that the absorption edge may appear to shift several hundred nanometers in wavelength for the same wafer material. As a further demonstration of the variability of the optical properties with thickness, visible red light is observed upon viewing a white light source through the 12 micron Si wafer. Utilizing the fact that the absorptivity, transmission, and reflection are together equal to unity, the absorptivity and corresponding luminescence spectra can be obtained. The resulting predicted photoluminescence curves exhibit a significant deviation from the expected curve at long wavelengths. The form and nature of this deviation is identical to that obtained using the FTIR based measurements shown in Fig. 4 and obtained by Band and Heller using other materials [23].

The absorption calculated from the above measurements represents the sum of the absorptivity which produces excited states (the quantum absorptivity) and the absorption which produces heat (the thermal absorptivity). One may, however, also estimate the quantum absorptivity from the photocurrent produced as a function

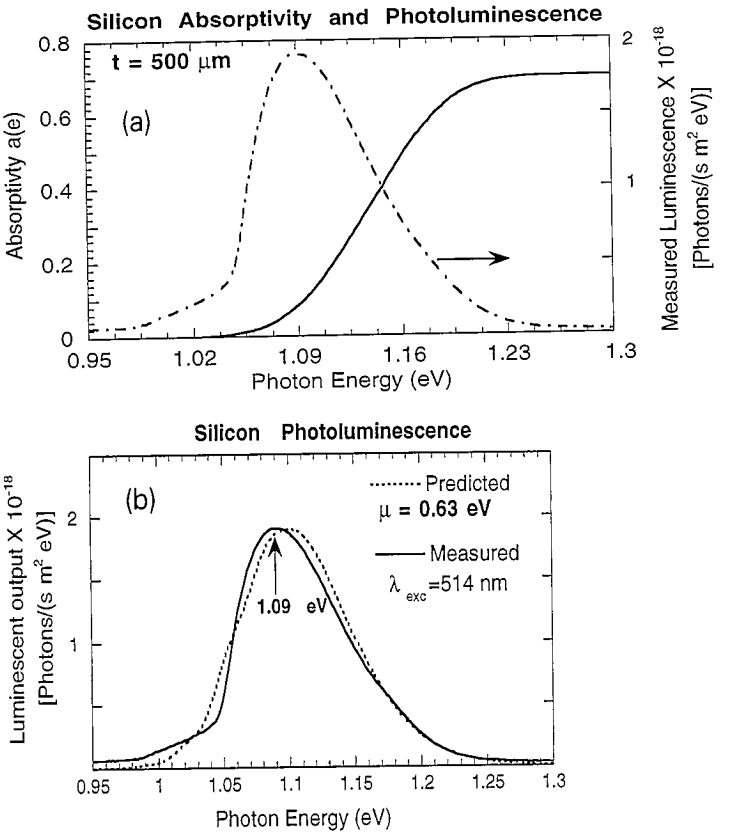

Fig. 2. (a) Silicon absorptivity calculated using the absorption coefficient [15], shown together with the photoluminescence measured in the present study. (b) Predicted and measured photoluminescence for silicon. The chemical potential used for the prediction is 0.63 eV.

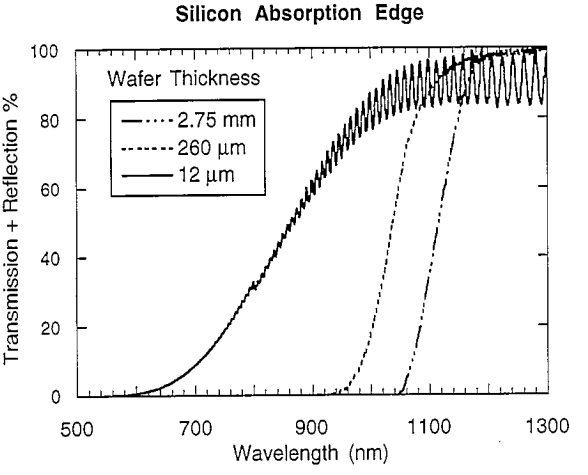

Fig. 3. Sum of Transmission and Reflection versus wavelength measured for three silicon wafers of different thicknesses using the set-up in Fig. 1a.

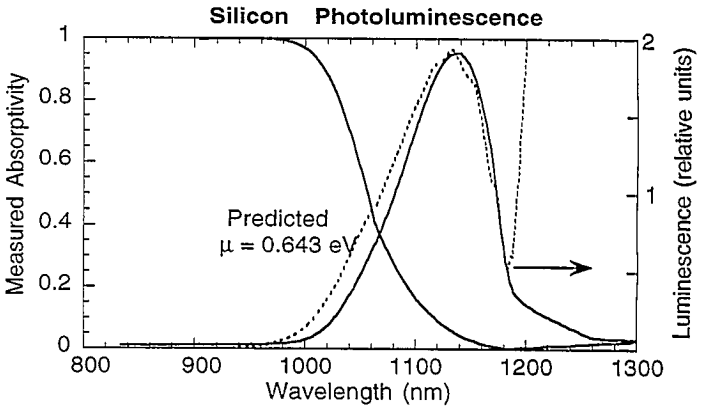

Fig. 4. Predicted Si photoluminescence (dashed line) obtained from an FTIR based measurement of absorptivity, together with the measured Si photoluminescence.

of wavelength, i.e., the IPCE. This measurement is shown together with the corresponding predicted photoluminescence in Fig. 5a, which is displayed with the experimental Si photoluminescence curve in Fig. 5b. This graph shows the predicted photoluminescence for a chemical potential of 0.63 and 0.615 eV. The voltage obtained from a solar cell possessing a p-type base layer of similar composition as the wafer described above is shown in Fig. 6, together it's AM 1.5 performance parameters (open-circuit voltage, V_{OC}, of 0.599 V, short-circuit current, I_{SC}, of 30.3 mA/cm^2). The predicted current–voltage curve is also displayed in Fig. 6, and utilizes the photoluminescence efficiency of 7×10^{-5} corresponding to the chemical potential in Figs. 2b, 5b [7]. The photocurrent is predicted from the product of the AM 1.5 photon flux and absorption obtained from Figs. 4 and 5a for the upper and lower prediction limits, respectively. As discussed in a previous paper, the photoluminescence from a solar cell should drastically decrease as the cell is cycled from the open to short-circuit conditions [7]. This was not observed in the present study, as shown in the time resolved measurements of Fig. 7. The time constant of the initial decay of the photoluminescence was found to be 27 ns. Similarly, the decay time constant for the oxide coated Si wafer was found to be 70 ns. These time constants are significantly smaller than were found using the same Si wafer and a time resolved microwave conductivity decay technique [24].

3.2. Results for photosynthesis

The digitized and re-processed literature values for the quantum yield and absorptivity for a typical plant leaf are displayed in Fig. 8. The total optical absorptivity shown in this figure is similar to a measurement made using the same experimental set-up described in Section 2.1. In Fig. 9, the product of these two optical quantities is shown, together with the experimental photoluminescence spectrum. The predicted photoluminescence, shown as a dashed line, is consistent

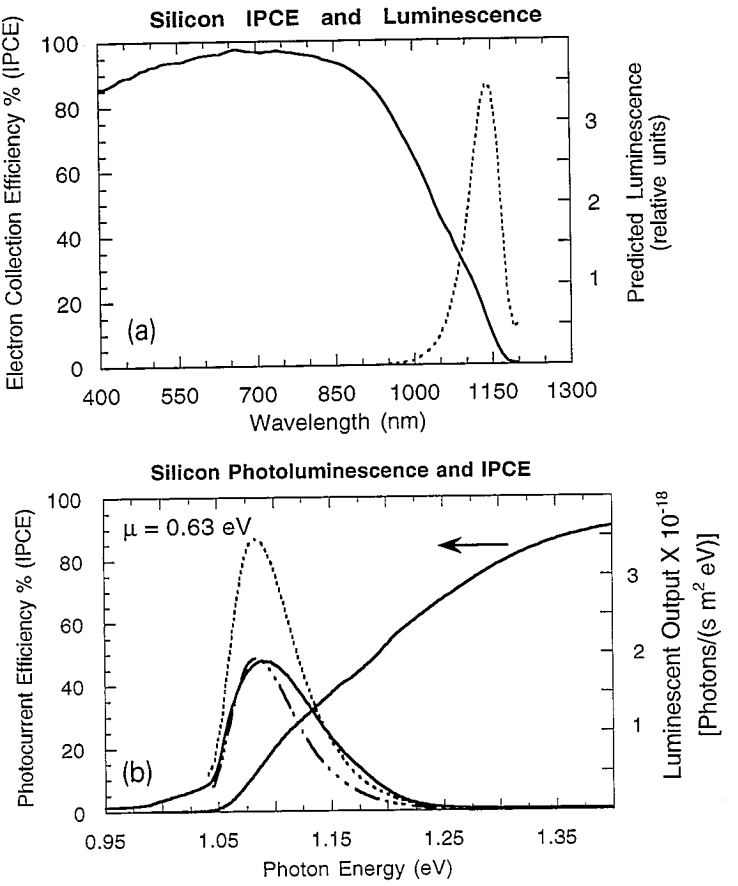

Fig. 5. (a) Experimental photocurrent spectrum for Si (solid line) and the corresponding predicted photoluminescence spectrum (dashed line). (b) Experimental (solid line) and predicted photoluminescence (dashed lines) calculated using the IPCE data and a chemical potential of 0.63 eV (higher dashed line) and 0.62 eV (lower dashed line).

with a chemical potential of 1.3 eV. The spectral characteristics of the experimental luminescence are those of Photosystem II, as well as Photosystem I. Photosystem II is thought to exhibit a luminescence spectrum, centered on 690 nm, that is stronger than Photosystem I. PSI is believed to exhibit a luminescence peak near 735 nm. The 735 nm peak is thought to originate from the peripheral antenna of PSI, or from chlorophyll phosphorescence [20,21]. The ratio of the two experimental photoluminescence peaks is highly variable, and dependent on the chlorophyll content and on physiological conditions [21]. The absorption of the intact leaf shown in Fig. 8 is also a composite of the absorption from PSII and PSI, since the long wavelength light used by PSI is not utilized to reduce NADP (Nicotinamide Adenine Dinucleotide Phosphate) or CO_2 without the concurrent operation of PSII [19]. This is a consequence of the series interconnection found between the

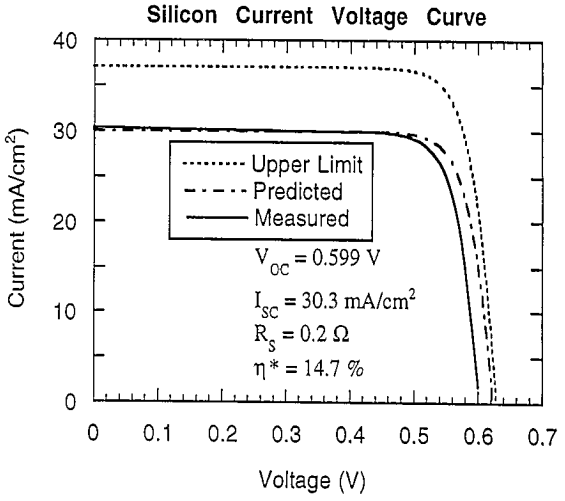

Fig. 6. Experimental (solid line) and calculated (dashed lines) current–voltage curve for the Si solar cell. The upper predicted curve (dashed line) uses the transmission and reflection data, while the lower (dashed-dotted line) utilizes the Si IPCE data.

two photosystems. Although the μ value of 1.3 eV was chosen to fit the observed photoluminescence yield of photosynthesis, this value was obtained by Ross who first applied this technique to photosynthesis [10].

As stated above, two interconnected photosystems operate in the photosynthesis found in green plants (PSII and PSI). The absorption data, taken from Joliot [22], for each of these two photosystems is shown in Figs. 10a and 10b, together with the predicted and measured luminescence from the present study. The luminescence is

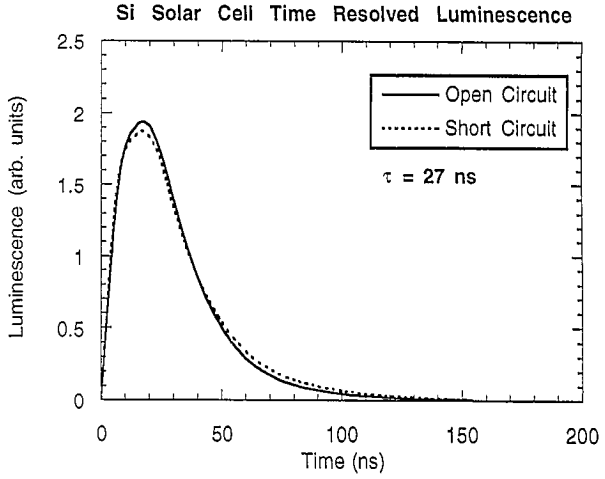

Fig. 7. Time resolved photoluminescence for the silicon solar cell at open-circuit and short-circuit conditions. The time constant for the decay is 27 ns.

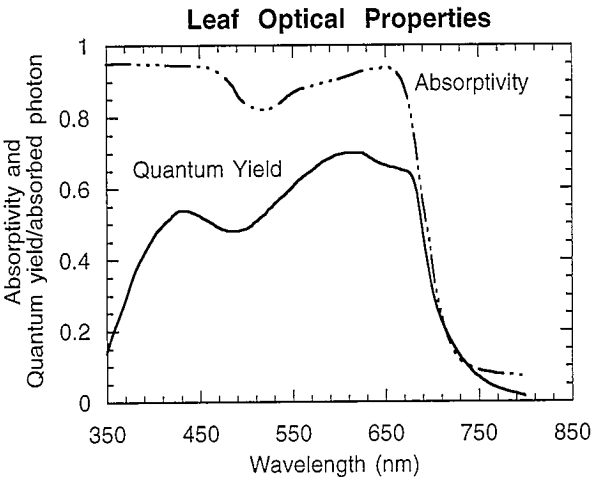

Fig. 8. Optical properties of a plant leaf obtained from a combination of literature sources [18].

also consistent with a chemical potential value of 1.3 ± 0.05 eV for both photosystems. This value is consistent with electrochemical based redox potentials determined for the various reduced compounds that are displayed on the energy band diagram (or "Z" scheme) of photosynthesis [19].

4. Discussion of results

The results of this study demonstrate that the photoluminescence spectrum for two typical solar converters can be predicted using measurement techniques and

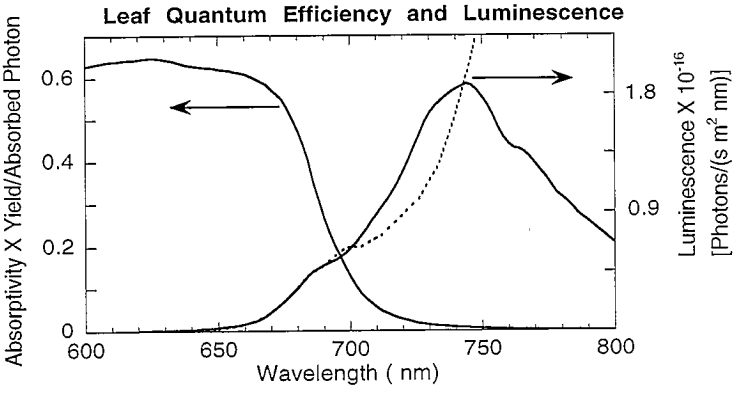

Fig. 9. Photoproduct versus wavelength for photosynthesis calculated from the product of the two plots shown in Fig. 8 (solid line at left). The resulting yield per incident photon is utilized as the absorptivity in the Generalized Planck equation in order to to generate the predicted photoluminescence spectrum (dashed line). The photoluminescence spectrum measured for a plant leaf is also shown (solid line at right). The integrated photoluminescence efficiency of the measured luminescence curve is 0.68% and the chemical potential used for the prediction is 1.3 eV.

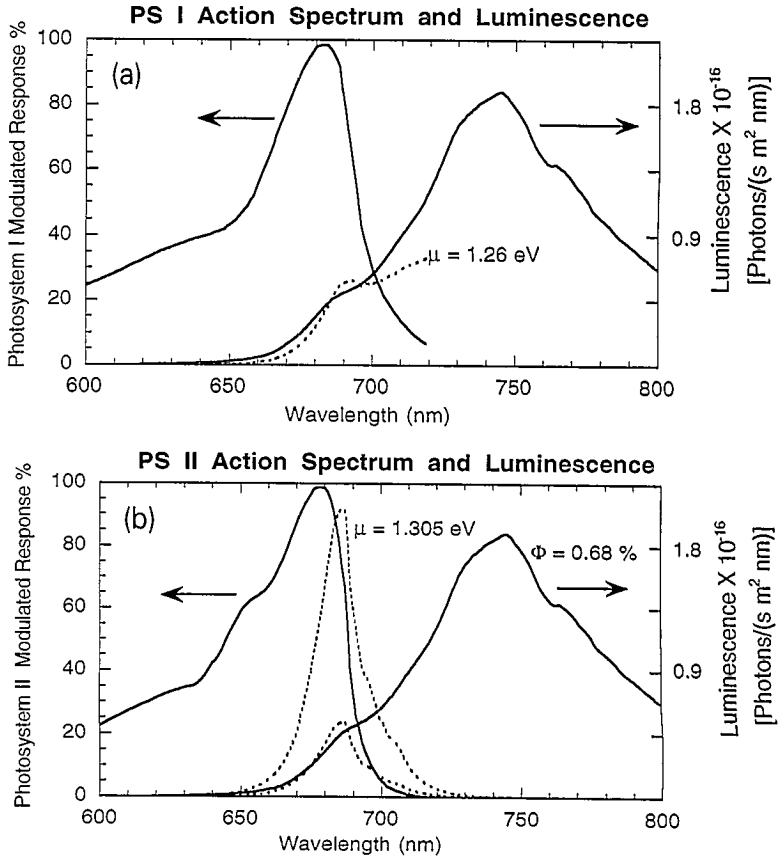

Fig. 10. Photosystem I, (a), and Photosystem II, (b), action spectra (solid line at left) together with the measured photoluminescence efficiency for the plant leaf (solid line at right) and predicted photoluminescence spectra (dashed line). Chemical potential values used to fit the theoretical curve to the experimental data are 1.26 eV for 10a and 1.3 and 1.26 eV for Fig. 10b.

equipment that are readily available to those in the field of solar conversion. Both the absorptivity and the induced photocurrent (or photo-product) spectrum can be used to estimate the quantum absorptivity necessary to predict the shape of the photoluminescence curve using the Generalized Planck equation. The chemical potential, μ, is in reasonable agreement with the values obtained using electrical techniques. The present study does, however, point out several important points relevant to the application of this theoretical formalism. The measured absorptivity is not necessarily equal to the quantum absorptivity used in the Generalized Planck equation. In the case of the spectrophotometer and FTIR based measurements, an overestimation of the absorption at long wavelengths may cause significant deviation from the expected curve. The cause of this deviation is due to the fact that the absorptivity is based on transmission data, for which the accuracy is difficult to maintain when detecting the loss of a small number of photons amidst a large signal. As Fig. 5b suggests, this problem may be alleviated by measuring the

small photocurrents produced by this weakly absorbed long wavelength light. Since the probability that an excited electron is collected may itself be a function of penetration depth, device structure, and the wavelength of light, the IPCE may also deviate from the quantum absorptivity. In order to separate these effects, models would have to be utilized which relate the IPCE to the absorption coefficient, device configuration, and ultimately, the quantum absorptivity [25–27].

As demonstrated by the measurements shown in Figs. 9–10a and 10b, which were performed on plant leaves, utilizing the photo-product yield does not guarantee a match to the measured photoluminescence curve. In addition to the difficulties discussed above, this system possesses two photosystems and several species, each with its own chemical potential and spectral distribution. In the case of silicon, there exists a chemical potential for the band to band excitation, as well as the chemical potential for the ***intra***-band absorption represented by free carrier (electron) absorption. In the case of photosynthesis, luminescent species may be present which dissipate some of the excitation energy and which do not participate in the formation of reduced NADP and CO_2. The underlying principle one learns from the two example quantum converters presented in this paper is that one must identify the source of the photoluminescence before applying the Generalized Planck equation. This is further exemplified by the time resolved results for silicon.

There have been many studies of other semiconductors regarding the photoluminescence as a function of operating voltage and current (see, for example, [28,29]). Many of these reports involved the use of the photoluminescence "dead" layer model which asserts that the photoluminescence depends exponentially on the width of the depletion layer. This model is employed since it is often observed that photoluminescence does not completely quench under operation at the short-circuit condition. This observation, and the results of Fig. 7, are in contradiction with predictions made using the Generalized Planck equation, since one expects a drastic change in photoluminescence as the voltage (or chemical potential) changes from open-circuit to zero. One possible reason for this discrepancy may be the use of the small spot size and the high power density employed in order to detect the weak signal. The photoluminescence efficiency for Si is in the range 10^{-4}–10^{-5}. Ideally, photoluminescence should be measured using temperature and irradiance conditions similar to those experienced by the device outdoors. Due to low photoluminescence efficiencies, these conditions are not always practical for studies of photoluminescence. A recent study by Saitoh et al. [30] established that the photoluminescence efficiency of Si may increase by several orders of magnitude as the excitation power of the laser is increased. At high illumination levels, the photogenerated electron concentration may exceed the intrinsic level (at the high injection condition). This may result in a flat band (or open-circuit) condition for the emission process before diffusion establishes the possibility of current extraction. An additional piece of information comes from time resolved microwave photoconductivity measurements of the same Si wafer [24]. The decay of the ***total*** excess electron concentration displayed a time constant several orders of magnitude larger than the photoluminescence signal displayed in Fig. 7. The small fraction of charge carriers which undergo radiative decay may do so at a faster rate

than those which non-radiatively decay. Clearly, a further examination of the photoluminescence properties of silicon as a function of illumination spot size, wavelength and power density is needed before the full interpretation of the Si time resolved photoluminescence results can be made.

5. Conclusions

In this paper, the quantum absorptivity estimated from transmission and Induced Photo-product measurements has been used to predict the performance of silicon and photosynthesis as quantum solar converters. It has been found that the practical application of the Generalized Planck equation is limited by the accuracy of the methods used to estimate the quantum absorptivity of the species directly involved in the production of an excited state. The predicted photoluminescence curves deviate from the experimental values in a manner dependent on the absorber material and measurement technique used to estimate the absorptivity. The chemical potentials obtained for silicon and for photosynthesis are consistent with the voltages and driving forces observed using other techniques. This could encourage the use of photoluminescence to explore and optimize solar converter materials. Before photoluminescence results can be converted from a strange and ambiguous signal to a useful characterization technique, however, further advances are necessary in measurement techniques and interpretation.

Acknowledgements

The author would like to thank Dr. Stephan Beeck of Instrument Systems GmbH for his help during the measurement of cw silicon photoluminescence. The assistance of Dr. M. Kunst and Dr. D. Herm of the Hahn Meitner Institute in Berlin is greatly appreciated and acknowledged in regards to time resolved measurements and interpretation.

References

[1] A.F. Haught, J. Solar Energy Eng. 106 (1984) 3.
[2] C. Winter, R. Sizman and L. Vant Hull, Solar Power Plants (Springer-Verlag, New York, 1991) Ch. 2.
[3] A. De Vos, Endoreversible Thermodynamics of Solar Energy Conversion (Oxford Science Publishers, Oxford, 1992) Ch. 6.
[4] A. Luque and G. Araujo, Physical limitations to photovoltaic conversion (Adam Hilger, New York, 1990) pp. 106–134.
[5] P.T. Landsberg, A. De Vos and P. Baruch, J. Phys.: Condens. Matter 3 (1991) 6415; P. Baruch, A. De Vos, P.T. Landsberg and J.F. Parrott, Sol. Energy Mater. Sol. Cells 36 (1995) 201.
[6] H. Ries and A. McEvoy, J. Photochem. Photobio. A: Chem. 59 (1991) 11.
[7] G. Smestad and H. Ries, Sol. Energy Mater. Sol. Cells 25 (1992) 51.
[8] K. Schick, E. Daub, S. Finkbeiner and P. Würfel, Appl. Phys. A 54 (1992) 109.

[9] P. Würfel, Sol. Energy Mater. Sol. Cells 29 (1993) 403.
[10] R.T. Ross and M. Calvin, Biophys. J. 7 (1967) 595.
[11] R.T. Ross and T. Hsiao, J. Appl. Phys. 48 (1977) 4783.
[12] R.T. Ross and J.M. Collins, J. Appl. Phys. 51 (1980) 4504.
[13] M. Archer and J. Bolton, J. Phys. Chem. 94 (1990) 8028.
[14] C. Barbero and R. Kötz, J. Electrochem. Soc. 140 (1993) 1.
[15] T. Tiedje, E. Yablonovitch, G. Cody and B. Brooks, IEEE Trans. Elec. Dev. ED-31 (1984) 711; for a more recent reference see M.J. Keevers and M.A. Green, Appl. Phys. Lett. 66 (1995) 174.
[16] J. Duffie and William Beckman, Solar Engineering of Thermal Processes 2nd Edition (Wiley, New York, 1991) pp. 926–931.
[17] Instrument Systems GmbH, Neumarkter Str. 83, 81673 München, Germany, (089) 454943-0.
[18] O.L. Lange and R.S. Nobel (Ed.), Physiological Plant Ecology I (Springer Verlag, New York, 1981) Ch. 2: Photosynthetically Active Radiation; T.J. Givnish, On the economy of Plant form and function (Cambridge University Press, New York, 1986) Ch. 2.
[19] P.S. Nobel, Biophysical Plant Physiology and Ecology (W.H. Freeman and Co., New York, 1983) pp. 238–353.
[20] W.R. Briggs, Photosynthesis (Alan R. Liss., Inc., New York, 1989) pp. 115–20.
[21] G.H. Krause and E. Weis, Annu. Rev. Plant Phys. Plant Mol. Biol. 42 (1991) 313–49; H.K. Lichtenthaler (Ed.), Applications of Chlorophyll Fluorescence (Kluwer Academic Publishers, Boston, 1988) Ch. 3.
[22] J. Bonner and J. Varner (Ed.), Plant Biochemistry (3rd Edition) (Academic Press, San Francisco, 1973) ch. 25.
[23] Y.B. Band and D.F. Heller, Phys. Rev. A 38 (1988) 1885.
[24] G. Smestad, M. Kunst and C. Vial, Sol. Energy Mater. Sol. Cells 26 (1992) 277.
[25] M.A. Green, High Efficiency Silicon Solar Cells (Trans Tech Publications, Switzerland, 1987) Ch. 3–7.
[26] A. Fahrenbruch and R. Bube, Fundamentals of Solar Cells (Academic Press, San Francisco, 1983) Ch. 5,7.
[27] C. Hu and R.M. White, Solar Cells From Basics to Advanced Systems, (McGraw Hill, San Francisco, 1983) Ch. 3.
[28] B. Smandek, G. Chmiel and H. Gerischer, Ber. Bunsenges. Phys. Chem. 93 (1989) 1094.
[29] R. Hollingsworth and J. Sites, J. Appl. Phys. 53 (1982) 5357.
[30] T. Saitoh, Y. Nishimoto, T. Sawada and H. Hasegawa, Jpn. J. Appl. Phys. 32 (1993) 272.